Application of Microcalorimeter Energy Measurement to Biopolymer Mass Spectrometry

M. W. Rabin, G. C. Hilton, and John M. Martinis

***Abstract*–We have performed electrospray ionization mass spectrometry using a magnetic sector mass spectrometer of proteins, detecting the ions with a normal-insulator-superconductor microcalorimeter detector. We emphasize the measurement of ion-impact energy as a way to obtain extra information that is unavailable in normal mass spectrometry. Energy measurements are used to discriminate against erroneous ion-strikes, to resolve ambiguities that cannot be resolved by normal mass spectrometry, and to illustrate some of the performance limits of the current detector design.**

***Index Terms*–electrospray ionization mass spectrometry (ESI-MS), microcalorimeter, mixture analysis, ion energy.**

I. Introduction

Mass spectrometry (MS) of high-mass biopolymers such as proteins, plastics and DNA is a difficult problem with applications in molecular biology, materials science, and medicine. The rewards for successfully developing a high-sensitivity MS using low-temperature detectors (LTDs) are potentially high, including the promise of ultra-fast determination of protein composition and DNA sequence. The use of LTDs based on superconducting devices as ion detectors for MS has three potential advantages: (1) high quantum efficiency (Q) for ion detection independent of ion mass (M); (2) extremely low noise due to low detector operating temperature (T<1K) and the use of SQUID read-out electronics; and (3) the measurement of ion-impact energy (E_I), which is proportional to ion-kinetic energy ($E_I \propto E_K$) and provides information that complements the spectrometer's determination of mass-to-charge ratio (M/Z, where Z is the number of elementary charges).[1] Previous results include E measurement of heavy proteins, assessments of quantum efficiency, analysis of oligonucleotides, and microorganism identification.[1-5]

In this article, we emphasize the use of E measurement as a tool for gaining information unavailable using a conventional ion detector. Our main point is that E measurement provides a new axis in the spectrum; it is no longer just an M/Z-spectrum (intensity vs. one variable), but it is an E- and M/Z-spectrum (intensity vs. two variables). To explain the significance of this, we must first briefly sketch some of the basics of biopolymer MS (Section II), showing how E measurement is especially useful for one technique, electrospray ionization mass spectrometry (ESI-MS). After describing our experimental set-up (Section III), including the MS and detector, we will present two results (Section IV). First we will use simple pulse processing and E spectra to determine ion M and Z in otherwise ambiguous cases. Second, we will use a combined E- and M/Z spectrum to show some of the limits of our detector's performance. We conclude with a discussion of the possible, future utility of E measurement, establishing criteria for energy resolution ($R_E=E/\Delta E$).

Manuscript received Sept. 19, 2000. This work was supported by the NIST Advanced Technology Program and MWR was supported by a National Research Council Postdoctoral Research Associateship.

All authors are with the National Institute of Standards and Technology, Boulder, CO, 80303 USA (telephone: 303-497-3021, email: rabin@boulder.nist.gov).

*These identifications do not imply recommendation or endorsement by NIST or the U.S. Government

II. Essential Features of Biopolymer MS

There are three essential steps common to all MS: the formation and launch of ions, their separation, and their detection. For heavy biopolymers, e.g. proteins with mass $M \gtrsim 10$ kDa**, the dominant means of producing intact, molecular ions are matrix assisted laser desorption/ionization (MALDI) and electrospray ionization (ESI).[7-9] MALDI produces intact, low-charge (Z=1 nearly always), molecular ions from a solid target in the MS vacuum using laser pulses. ESI produces intact, high-charge (about one charge unit per every few thousand Da), molecular ions from a liquid sample source. After formation, the ions are accelerated and separated either electromagnetically (e.g. by a magnet or a quadrapolar RF field) or temporally, i.e. by their time-of-flight (TOF). Since ion acceleration in vacuum in an electromagnetic field is inversely proportional to M/Z, all MSs separate different values of M/Z; they do not separate purely in M unless Z=1. Once separated, the ions are detected, most commonly with a charge-cascade device, such as a micro-channel plate (MCP).

Most biopolymer MS is done by MALDI-TOF-MS because samples are easy to prepare, MALDI mates well with TOF, and TOF has inherently high sensitivity. TOF is a pulsed method, and for each pulse, an entire M/Z-spectrum can be collected without scanning any electromagnetic parameters. With Z=1, the spectra are also easy to interpret. But in the high-mass

** Da = Dalton = 1 atomic mass unit = 1.67×10^{-27} kg

range (M>100kDa), the M/Z-spectrum is spread out into a region with two problems. First, there is a dramatic decrease of mass-to-charge-ratio resolution ($R_{M/Z}=(M/Z)/\Delta(M/Z)$) inherent in the ion formation and launch; the best MALDI-TOF spectra for DNA and proteins in this mass-range have $R_{M/Z}$ of only $\lesssim$100.[11-12] This problem has so-far defied solution, and is significant for some important potential applications, e.g. measuring the mass-distribution function of some synthetic polymers and sequencing DNA. Low $R_{M/Z}$ is considered to be the performance limiting parameter in high-mass biopolymer MS. The second drawback of MALDI-TOF is the rapid drop in quantum efficiency (Q) of standard ion detectors for M/Z>50 kDa, reducing sensitivity by $\gtrsim$100 relative to the low-mass range.[10] The MS community does not see this drop in Q as a serious obstacle; chemists are willing to detect <1% of their ions from M~100 kDa to 500 kDa. If sensitivity becomes the compelling issue, perhaps as the upper end of the mass range grows beyond 1 MDa or $R_{M/Z}$ improves, the M-independent Q of LTDs would have greater applicability.

The second major ionization method, ESI, is becoming increasingly popular, especially in the field of proteomics, the determination of the complete set of proteins expressed (as opposed to genetically encoded) by a cell or organism under a specified set of conditions.[12] ESI is potentially the most sensitive biopolymer ionization system, with the added virtue that it can directly couple to liquid sample sources, like the output of a liquid chromatograph. Furthermore, ESI produces multiply charged ions in the range M/Z~1000 to 5000 Da, hence easily staying within the M/Z range of typical spectrometers and retaining very high $R_{M/Z}$ for all M. ESI couples well to either TOF spectrometers (using an orthogonal geometry) or scanning spectrometers, like RF quadrapoles. But ESI produces a distribution of charge states for each analyte, e.g. Z=5 to 10 for a modest protein (M~20kDa) or Z=−25 to −35 for a ~300 nucleotide-long single-stranded DNA molecule (M~100 kDa). The ESI-MS M/Z spectrum for a single biopolymer therefore consists of many peaks. Since the peaks of all of the charge states for all biopolymers fall into the same M/Z range, the M/Z spectrum of a complex mixture (e.g. 7 different proteins) is a dense set of overlapping peaks. Though there is sophisticated software to deconvolve ESI M/Z spectra, it produces spurious results and misses components when there are more than about 5 analytes. The direct ESI-MS analysis of complex mixtures with typical spectrometers is therefore impossible because the M/Z spectrum alone is too congested.[13] This difficulty directly affects the ESI-MS determination of proteomes, synthetic polymer mass distribution functions, and nucleic acid sequences; successful analysis in each of these cases requires some type of (often difficult or time-consuming) chromatography to precede ESI-MS. Significant research is underway to alleviate this problem by reducing charge states, but this might have a substantial cost in sensitivity.[14]

The unique ability of our detectors to measure the ion-impact energy (E) of individual ions can potentially moderate this problem. Since $E \propto E_K = Z\,e\,V$, where e is the proton charge and V is the MS accelerating voltage, a sufficiently precise measurement of E and M/Z determines Z and M. Therefore we can make a difficult-to-understand M/Z-spectrum of a complex mixture easier to interpret. One of our aims is to analyze DNA ladder samples and distinguish the components of the mixture. For one of the main techniques in biopolymer analysis, ESI-MS, our detectors have a special advantage that may provide information that is otherwise impossible to obtain.

III. Experimental

A. Mass Spectrometry

We have performed ESI-MS analyses of proteins and protein mixtures. All chemicals (bought from SIGMA)* were dissolved in a DI-water:methanol:acetic acid (50:50:3) solution without further purification. The ESI source (Analytica of Branford)* follows the classic design of Fenn[6], and injects ions into a magnetic-sector mass spectrometer (JEOL HX110)*. The injection rate into the ESI atmospheric chamber was ~8 to 30 nl/s (0.5 to 2 µl/min), and a counter current flow of N_2 gas increased the solvent evaporation rate from the electrosprayed droplets. The ESI needle was either a fused silica capillary (50µm i.d.) or a stainless steel capillary (100µm i.d.) operated at 2000 to 3000 Volts. The needle was ~1cm away from the inlet of the MS. This inlet was the metalized-end of a glass capillary (500 µm i.d.), which was held at ground potential. The glass capillary acts as the first step in a differential pumping manifold designed to transfer the ions from the atmospheric-pressure region where they are created into the MS acceleration region, where the pressure is roughly 1 mPa (~10^{-5} Torr). Ions are then accelerated through V=4000 Volts into a cylindrical electric field and then into a magnetic field. Electrostatic quadrapole lenses are used to focus the ion beam onto an adjustable collector slit, whose size determines $R_{M/Z}$. Typically $R_{M/Z}$=1000 to 3000. M/Z spectra are obtained by

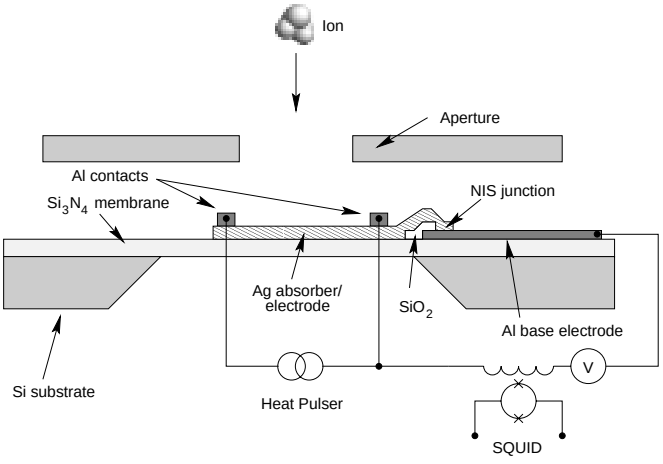

Fig. 1. Cross-sectional view of NIS microcalorimeter, showing final aperture, Ag absorber, NIS junction, Si_3N_4 membrane, and series-array SQUID readout electronics.

sweeping the magnetic field over a range corresponding to M/Z=1000 Da to 5000 Da. The magnetic field, hence M/Z through calibration, was monitored with a standard Hall probe. The spectrometer is equipped with two detectors. The first is a conventional charge-cascade detector: a conversion dynode and electron multiplier. The second is our cryogenic detector: a normal-insulator-superconductor (NIS) microcalorimeter (Fig. 1). We can electrostatically switch between the two detectors. An electrostatic double quadrapole and deflector plates concentrate the ion beam onto the NIS.

B. NIS-Microcalorimeter Detector

Our detector is an NIS microcalorimeter, shown in cross section in Fig. 1, and is based on designs that have been fully described previously [2]. Microcalorimeters measure the ion by absorbing and thermalizing a quantum of energy, causing a temperature increase (ΔT) of an absorber, which has a small heat capacity (C) . The heat then escapes through a thermal conductance (G) to a cold thermal bath (~100mk). A sensitive thermometer measures ΔT, which is proportional to the absorbed energy. When an ion strikes the NIS's Ag absorber (350 µm x 350 µm x 200 nm), a fraction of the ion's E_K is thermalized, depositing energy E into the electrons of the Ag film. The subsequent ΔT produces a current pulse $\Delta I(t)$ in the voltage-biased NIS junction. In this case, the absorber is an integral part of the thermometer, and $\Delta I(t)$ is measured using a low-noise 1 MHz-bandwidth series-array SQUID amplifier.[15] The detector's effective fall-time constant (including electrothermal feedback) is ~12µs, and the energy resolution for 6keV X-rays is ~100 eV. After digitally sampling and filtering each pulse, we extract the pulse height (h); $h \propto E_I \propto E_K$.

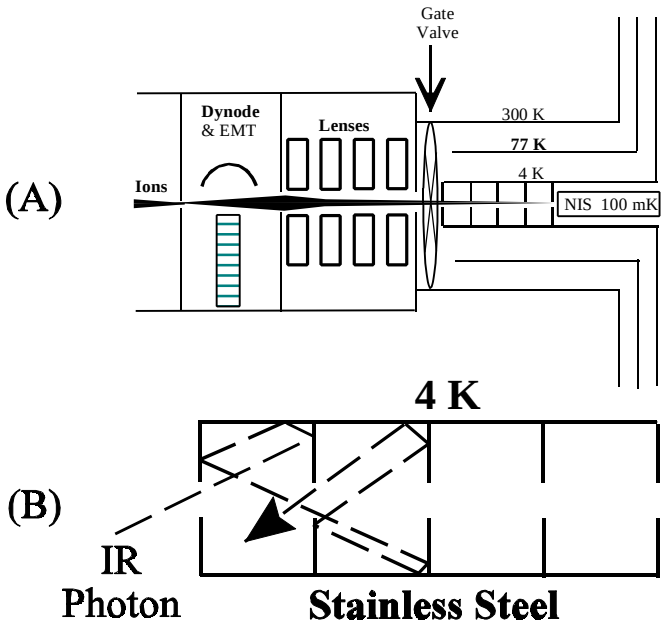

Fig. 2. Schematic of room-temperature to low-temperature interface. (A) Overview showing thermal shields (77K and 4K) and ion-optical lenses concentrating the beam onto the NIS at T~100 mK. (B) Close-up of 4K IR light trap. Stray light must bounce many times off of interior baffles to pass through, with an ~0.5 chance of absorption at each bounce. The holes in the baffles have a 2 mm diameter and the 4K light trap is 150 mm long.

C. Room-Temperature-to-Low-Temperature Interface

One unique feature required for these experiments is the connection of a room-temperature spectrometer that produces massive, charge particles with a T~100 mK detection system. Unlike X-ray and far infrared light measurements using LTDs, there can be no window with solid panes blocking the 300K (10µm) thermal radiation. There must be a hole for the ions to pass through. The design of the interface between the 300K and 100mK regions must balance the desire to open up the hole as wide as possible to admit the maximum ion flux and the need to close the hole to prevent radiative power-loading of the detector. Our compromise design is a simple set of 4K stainless steel baffles, illustrated in Fig. 2. Each baffle has a 2 mm hole centered on the ion-optical axis. Though line of sight radiation passes through, light that is only slightly off-axis must bounce several times among the 4K baffles. Assuming an emissivity of ~0.5, these baffles reduce the heat-load enough to prevent significant power-loading of the detector. All materials used in or around the ion beam, especially baffles and apertures, must be metallic conductors with well defined paths to electrical ground; other materials (e.g. black paints) or floating metals will become charged by the ion beam. These charged components will erratically steer the ion beam away from the ion-optical axis and away from the detector.

IV. Results

A. Pulse Processing to Discard Erroneous Ion-Strikes

Using the current NIS-ion-detector design, we usually find a bimodal distribution in pulse heights (h) at fixed M/Z, like that shown in Fig. 3A. In this ESI-MS analysis of myoglobin II (an M=6210 Da digestion product of myoglobin) at M/Z=1553 Da, we find a minor peak at h~0.08 (arbitrary units) and a major peak at h~0.3. The major peak corresponds to the expected Z=+4 charge state, and is consistent with the spectra from other compounds. But the pulse-heights in the minor peak are close to the value expected for Z=+1 ions, so the minor peak might be due to the presence of another species with M=1553. A simple analysis of the shape of the current pulses ($\Delta I(t)$) and the pulse-height histogram shows that the minor (lower-energy) peak is composed of ion strikes on the silicon-nitride membrane, not ions of another species.

The pulse-shape analysis, shown in Fig. 3B, proceeds as follows. All the pulses in the bin around h=0.08 are averaged, normalized, and time-shifted so that $p(t)=\langle \Delta I(t) \rangle / \langle h \rangle$ and $p(0)=1$; the same procedure is performed at h=0.32. The normalization and time-shift allow us to directly compare the

rate of heat-flow into- and out of the microcalorimeter independent of pulse height and trigger threshold. It is clear that the rise and fall of the h=0.08 pulses is slower than that of the h=0.32 pulses. Furthermore, the fall of the h=0.32 pulses very nearly matches that of thermal heat pulses. The same rise- and fall behavior is found using nearby bins. From these results, we conclude that the minor peak is composed of ion-strikes on the silicon nitride membrane. When an ion strikes the membrane, the thermal energy will diffuse more slowly into- and out of the electrons in the N layer of the junction, so we expect both the pulse rise-time and fall-time of membrane strikes to be slower than absorber strikes. Furthermore, the heat-leak to the Si surrounding the membrane will reduce the amount of heat that reaches the N-layer electrons, so the pulse height of membrane strikes will be less than that of absorber strikes. The presence of membrane strikes indicates that the final aperture (300µm diameter) is too far away from the detector, and some ions will pass through the aperture on trajectories that will intersect the membrane and not the absorber. It is also possible that some ions are glancing off the aperture, losing energy, and striking the membrane. We have found the fraction of membrane strikes to depend on the setting of the final electrostatic deflectors that aim the ion-beam onto the detector, further supporting the inference that our aperture needs to be closer to the detector to eliminate membrane strikes.

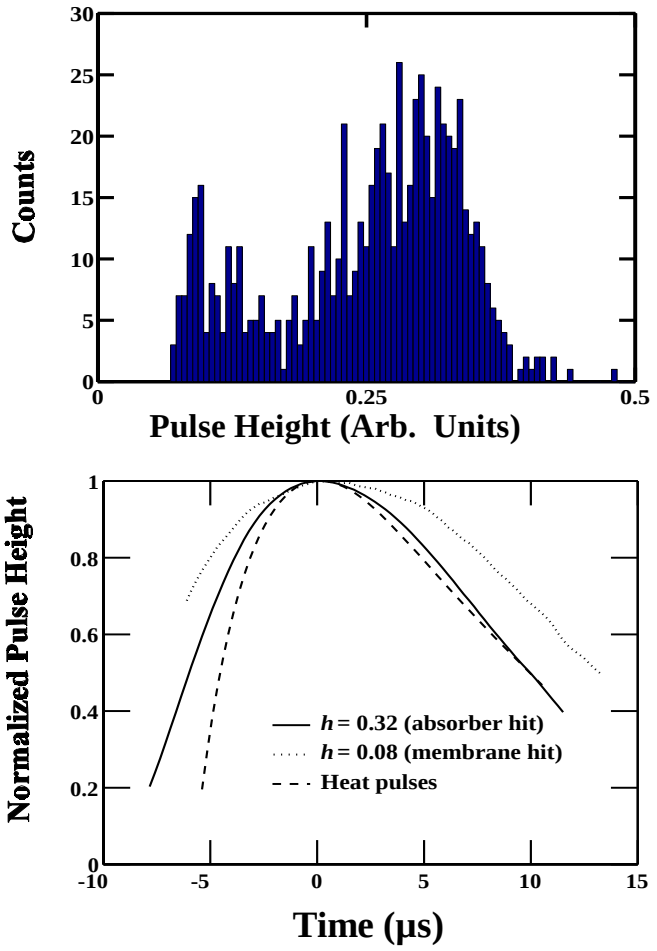

Fig. 3. Pulse-height and pulse-shape analysis for myoglobin II at fixed M/Z=1553 Da. (A) Pulse-height (h) histogram. (B) Averaged, normalized pulses, $p(t)$, for h=0.08 (top), h=0.32 (middle), and resistive heating (bottom).

B. E spectra to Identify Doubly-Charged Dimers

Using only the M/Z-spectrum, it is sometimes impossible to unambiguously attribute some M/Z-peaks to one species if the sample contains monomers (M=M_1), dimers (M=2 M_1), trimers (M=3M_1), etc, because the singly charged monomer, doubly charged dimer, triply charged trimer, etc. all have the same M/Z That is, M_1/Z=2M_1/2Z=3M_1/3Z=... Fig. 4 illustrates how this ambiguity is resolved using E measurement for the protein lysozyme, with mass M_{LYS}=14300 Da. The E spectrum is for a narrow range around M/Z=3575 Da, with $\Delta(M/Z)$~10 Da. This M/Z-range corresponds to the +4 monomer, +8 dimer, etc. The E spectrum divides into four well separated regions. (a) h<0.07; (b) 0.12<h<0.17, (c) 0.24<h<0.29, and (d) h>0.51. By using the pulse shape and pulse-height correlation outlined in the previous section, we can disregard the 21 pulses in region (a) as membrane strikes. The major peak, region (b), contains 67 pulses with mean pulse height h_b=0.135. The minor peak, region (c), contains 14 pulses with mean pulse height h_c=0.273. The 5 pulses at high-energy, region (d), do not form a well-defined peak, but have a mean pulse height of h_d=0.551. The mean pulse heights are nearly in integer ratios: h_c/h_b=2.0 and h_d/h_b=4.1 and h_d/h_c=2.0. Since h_b matches the expected value for the +4 charge state, the integer ratios of the peak heights suggest that the minor peak (c) is due to lysozyme dimers and that the high-energy region (d) is possibly due to lysozyme

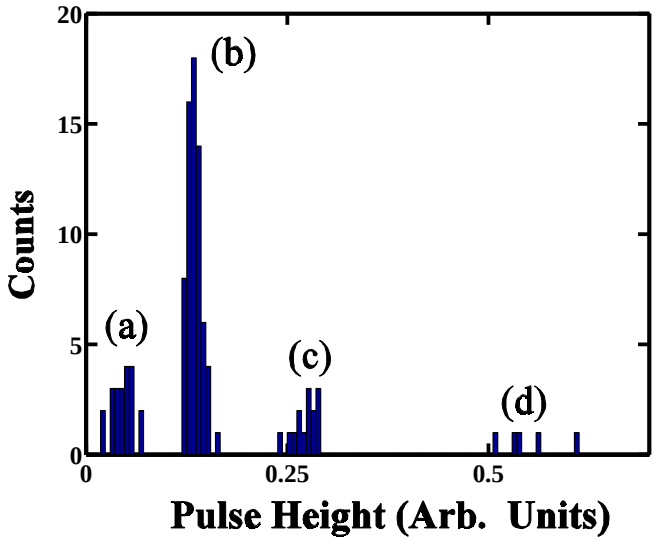

Fig. 4. Pulse-height (h) histogram for lysozyme at fixed M/Z=3575 Da showing (a) membrane strikes, (b) a major peak due to the lysozyme monomer with Z=+4, (c) a minor peak lysozyme dimer with Z=+8, and (d) a higher energy group of ions possibly due to lysozyme quadramers with Z=+16.

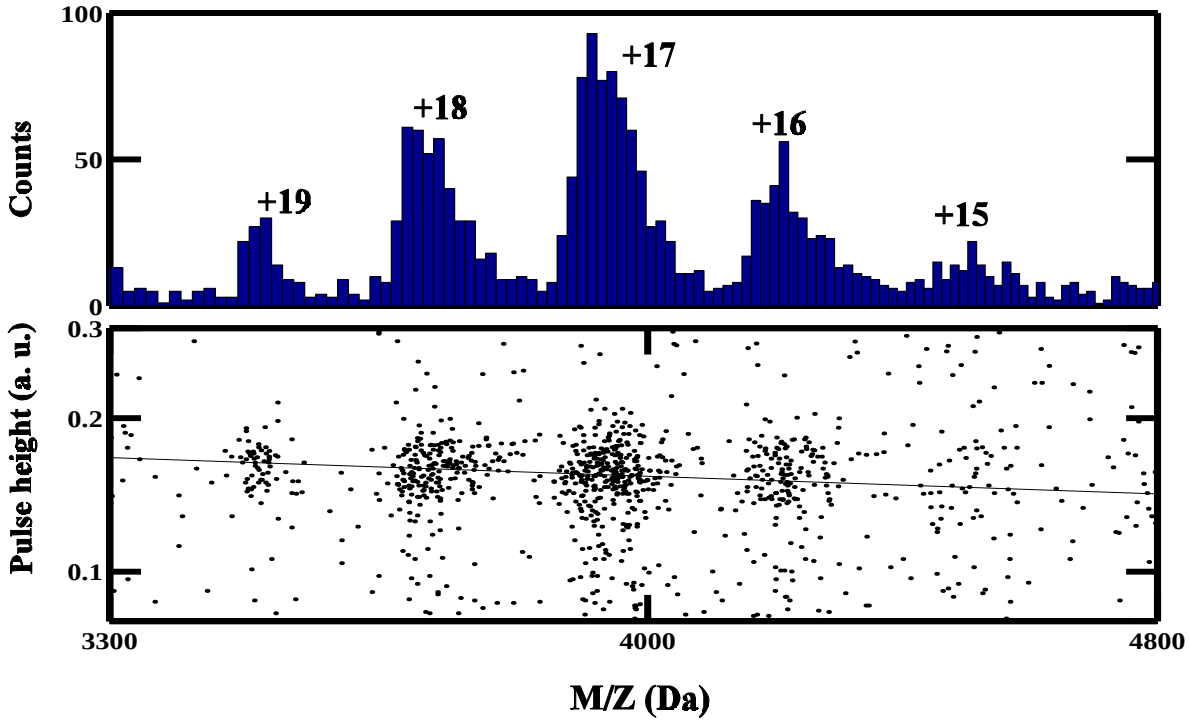

Fig. 5. Combined *M/Z*- and *E* spectrum for bovine serum albumin on log-log axes.

quadramers. The presence of the lysozyme dimer is confirmed by similar *Z*:2*Z* pairs of peaks corresponding to the +3:+6 and +5:+10 charge states and by peaks at $M/Z=2M_{LYS}/9$ and $2M_{LYS}/7$. No such confirmation is found for the lysozyme quadramer.

It is important to note three features of the foregoing analysis of the *E* spectrum at fixed *M/Z*. First, the spaces between the four regions (a)-(d) are empty, reflecting the low noise of the detector; all of the pulses in Fig. 4 should be regarded as real ion strikes, not noise counts, which are effectively zero. Second, given the very few dimer- and putative quadramer ion strikes, it is important to look for confirmation in other regions of the *M/Z*- and *E* spectrum. And, third, this type of analysis is impossible using a conventional MS detector.

C. Combined *M/Z*- and *E* spectrum and Large Z

We can combine *M/Z*- and *E* spectra and measure high charge states ($Z\sim20$), as shown in Fig. 5, the ESI-MS spectra of bovine serum albumin (BSA, $M_{BSA}\sim66$kDa). The upper portion shows the conventional *M/Z* spectrum (logarithmic horizontal axis); the lower portion shows a scatter plot of *h* vs. *M/Z*, (both on logarithmic axes). Each small dot corresponds to a single ion strike, and the measurement of both *h* and *M/Z* for that ion. The breadth of the *M/Z*-peaks is due to chemical noise and adduct formation (e.g. Na), which we should be able to reduce in subsequent experiments by using cleaner ESI methods and purification. In the *M/Z*-spectrum, the +15 to +19 BSA charge states are apparent, with possible, small peaks at +21 and +15. The scatter plot shows shot-groups of ion strikes corresponding to each of the +15 to +19 charge states along with the usual, low-energy membrane strikes. These results are the largest *Z* values and highest ion energies, E=60 to 76 keV, so far measured with a LTD ion detector in an MS experiment. The breadth of the energy distribution (vertical scatter) within any shot group is large; using the *E* spectra for $Z=+17$ ($M/Z\sim3900$) shot-group, we estimate the energy resolution at $R_E\sim5$. This low R_E is clearly insufficient for making unambiguous charge attribution based solely on *E* measurement because the energy distributions of neighboring charges (e.g. $Z=16$ and $Z=17$) overlap. But the overall trend is clear, with the mean peak heights for each charge state decreasing with *M/Z*. For a linear detector, $h\propto E\propto Z$, therefore $\ln(h)=\ln(k)+\ln(M)-\ln(M/Z)$, where *k* is a constant. We expect the shot-group centers corresponding to a common mass (fixed *M*) to fall on a line of slope -1. From the least-squares-best-fit line through the shot-group centers in Fig. 5, we extract a slope of -0.4, which is a measure of the nonlinearity of our detector near $E\sim$ 70 keV. Each shot-group center is the maximum in the *M/Z* spectrum and the maximum in the *h* spectrum for a major peaks ($Z=+16$ to +17). Though the detector enters the nonlinear regime for these high energies, pulse shapes show that the detector has not saturated. Though these results are plagued by chemical noise and insufficient R_E to unambiguously determine *Z*, they illustrate the technique of using a combined *M/Z*- and *E* spectrum.

V. Future Work on *E* measurement

The preceding sections demonstrated how *E* measurement can be used to gain more information in MS, how that information can be applied to ESI-MS of proteins, and what some of the current limits on *E* measurement are. For *E* measurement to be useful to the mass spectrometrist, R_E must increase. In our next detector design, we will try to increase R_E by changing the absorbing layer to increase the fraction of E_K deposited in the absorber, which might reduce the variance in E_I.

We will now establish target values for R_E to be useful in the specific problem of DNA sequencing by MS. This problem is important because successful DNA sequencing by MS could be more than 100 times faster than current electrophoretic methods. To set some R_E-criterion for *E* measurement to be useful, we consider the specific problem of DNA sequencing. To successfully compete with electrophoretic methods, MS requires a mass range corresponding to DNA fragment lengths of N~300 to 1000 nucleotides (nt), i.e. M~100 to 300 kDa, and the necessary resolution to distinguish the presence and absence of consecutive nucleotides with mass difference ΔM~300 Da. On a statistical basis, we can attempt to separate peaks using the two axes, *M/Z* and *E*, of our spectrum; this is analogous to distinguishing spots in two-dimensional gel-electrophoresis of proteins or nucleic acids. We have conducted some simple simulations of ESI-MS DNA sequencing with an energy resolving detector; the critical ingredients for the simulation are R_E, $R_{M/Z}$, and N. The results show that for N=300 nt, $R_{M/Z}$=1000, and R_E=30, the peaks of the regular *M/Z*-spectrum are unresolved, but all the peaks of the two-dimensional *M/Z*- and *E* spectrum are easily resolved by eye. At R_E=30, ~50% of the peaks are baseline resolved; at R_E=60, ~90% are. Clearly, the critical parameter for the success of this approach is R_E. To compete in mass range with current MALDI-TOF DNA sequencing experiments, we need only R_E~10 to 20; to compete in mass range with electrophoresis at N~300, we need $R_E \gtrsim 30$. Though these simulations set criteria for R_E, other criteria such as speed and effective area must also be met for microcalorimeter detectors to have significant utility to the MS community.

Acknowledgment

We thank Prof. Lloyd Smith of the University of Wisconsin for his thoughts on MALDI-TOF-MS and Prof. Klaus Biemann and MIT for the donation of the mass spectrometer used in this work.

References

[1] M. Frank, S. E. Labov, G. Westmacot, and W. H. Benner, "Energy-sensitive cryogenic detectors for high-mass biomolecule mass spectrometry," *Mass Spectrometry Reviews*, vol. 18, pp. 155-186, 1999. A useful review with complete references.

[2] G. C. Hilton, et al, "Impact energy measurement in time-of-flight mass spectrometry with cryogenic microcalorimeters," *Nature*, vol. 391, pp.672-675, Feb. 1998.

[3] D. Twerenbold, *et al*, *Applied Physics Letters*, vol. 68, pp. 3503, 1996.

[4] G. Gervasio, *et al*, "Aluminium junctions as macromolecule detectors and comparison with ionizing detectors," *Nuclear Instruments and Methods in Physics Research A*, vol. 444, pp. 389-394, 2000.

[5] J. N. Ullom, *et al*, "Identification of microorganisms using superconducting tunnel junctions and time-of-flight mass spectrometry," *Nuclear Instruments and Methods in Physics Research A*, vol. 444, pp. 385-388, 2000.

[6] J. B. Fenn, M. Mann, C. K. Meng, S. F. Wong, C. M. Whitehouse, "Electrospray ionization for mass spectrometry of large biomolecules,"*Science*, vol. 246, pp. 64-71, 6 Oct. 1989.

[7] M. W. Senko and F. W. McLafferty, "Mass spectrometry of macromolecules: has its time now come?" *Annual Review of Biophysics and Biomolecular Structure*, vol. 23, pp. 763-765, 1994.

[8] R. D. Smith, *et al*, "Principles and practice of electrospray ionization mass spectrometry for large polypeptides and proteins," *Mass Spectrometry Reviews*, vol. 10, pp. 359-451, 1992.

[9] E. Nordhoff, F. Kirkpekar, and P. Roepstorff, "Mass Spectrometry of Nucleic Acids," *Mass Spectrometry Reviews*, vol.15, pp. 67-138, 1997.

[10] G. Westmacott, M. Frank, S.E. Labov, W.H. Brenner, "Using a superconducting tunnel junction detector to measure the secondary electron emission efficiency for a MCP detector bombarded by large molecular ions," submitted to *Rapid Communications in Mass Spectrometry*.

[11] N. I. Taranenko, *et al*, "Sequencing DNA using mass spectrometry for ladder detection," *Nucleic Acid Research*, vol. 26, pp. 2488-2490, 1998.

[12] J. R. Yates, "Mass Spectrometry in the Age of the Proteome," *Journal of Mass Spectrometry*, vol. 33, pp. 1-19, Jan. 1998.

[13] M. Scalf, M. S. Westphall, J. Krause, S. L Kaufman, and L. M. Smith, "Controlling Charge States of Large Ions," *Science*, vol. 283, pp. 194-197, 8 Jan. 1999.

[14] M. Scalf, M. S. Westphall, and Lloyd M. Smith, "Charge Reduction Electrospray Mass Spectrometry," *Analytical Chemistry*, vol. 72, pp. 52-60, 1 Jan. 2000.

[15] R. P. Welty and J. M. Martinis, "A series array of dc SQUIDs," *IEEE Transactions on Magnetics*, vol. 27, pp. 2924-2926, 1991.